ANALYSIS OF SEGMENTAL TUNNEL LININGS AT EXTREME LEVELS OF OVALISATION CAUSED BY SOIL EROSION

R. Sturt, G. Montalbini, H-I. Jung
Arup, UK

ABSTRACT: A novel numerical modelling method is proposed in which each joint of a segmental tunnel lining is represented by a series of discrete elements distributed through the segment thickness. Each element represents a particular zone of the joint face or a component such as a bolt or gasket, with force–displacement properties derived from detailed nonlinear finite element (FE) models of the joints. The modelling method enables interpretation of joint damage states and remains applicable beyond the deformation range typically considered in design, while enabling efficient analysis of three-dimensional multi-ring models. The method is applied to the NakDong Tunnel, part of which collapsed in 2020 following loss of horizontal support due to soil erosion. Example analyses are presented that explore the sensitivity of the tunnel ovalisation response to the circumferential joint design. While quantitative results are specific to the NakDong Tunnel, the modelling approach is applicable to segmental tunnels in general.

1. INTRODUCTION

A section of the newly constructed NakDong Tunnel, which forms part of the Bujeon–Masan Railway in Korea, collapsed in March 2020 following erosion of surrounding soil caused by water inflow towards a leaking cross passage. Official investigations concluded that the segmental lining design was not the direct cause of collapse. Nevertheless, the behaviour of the tunnel lining offers a potential learning opportunity for the worldwide tunnel design community due to the scarcity of data on the behaviour of segmental tunnel linings at deformation levels greater than those which are typically considered during design. Along with the collapsed sections, site investigation revealed several rings that had not collapsed despite ovalisation deformation greater than 350mm (4.5% of tunnel diameter). The circumstances of the collapse, findings from the site investigation, and detailed finite element modelling of the segment joints have been reported previously (Seol et al., 2022, Sturt et al., 2025). The present paper builds on that work by deriving simplified joint models suitable for efficient multi-ring analysis of events that induce large deformation of segmental tunnels.

Conventional tunnel design commonly uses two-dimensional beam–spring models, with joint effects represented by stiffness reductions (Wood, 1975) or by joint elements with force-dependent moment–rotation relationships. Three-dimensional multi-ring models with discrete joint elements can capture staggered joint effects more realistically (Moreno-Martinez 2020) but if these are to be applied to large deformation scenarios, they require joint models that remain valid under large rotation and slip conditions. Single-element joint representations struggle to capture the complex interaction of localised mechanisms such as concrete crushing, bolt yielding and gap closure under a range of loading scenarios. This paper proposes a novel solution in which the overall joint response is built up from a number of separate spring-like discrete elements, each of which represents a particular component or zone of the joint face and has input data derived from the force-displacement response of the equivalent component or zone of a detailed finite element model.

1.1 MODELLING STRATEGY

Numerical modelling has played an important role in understanding the collapse mechanism of the NakDong Tunnel and in planning the recovery works. To enable analysis of multiple-ring tunnel models within practical timeframes, simplified modelling methods are required that balance accuracy with computational efficiency. The detailed finite element models (Sturt et al., 2025) represent only a single joint but require 5–10 hours to run using 32 processors, making whole-tunnel modelling impractical. By contrast, the simplified eleven-ring models described herein require approximately 30 minutes on the

same computing set-up. All analyses were carried out using LS-DYNA (Ansys, 2023), a general-purpose nonlinear finite element analysis program.

Since deformation and failure of the tunnel lining are concentrated primarily in the joints, it is essential that the simplified model captures joint moment–rotation and shear force–displacement behaviour accurately up to failure. Analytical methods cannot readily represent the complex nonlinear behaviour involved, and physical testing was not feasible within the project timeframe. Therefore, the joint properties adopted in the simplified model were derived from detailed finite element analyses and cross-checked against observed damage in the collapsed tunnel (Sturt et al., 2025), see Figure 1 top images.

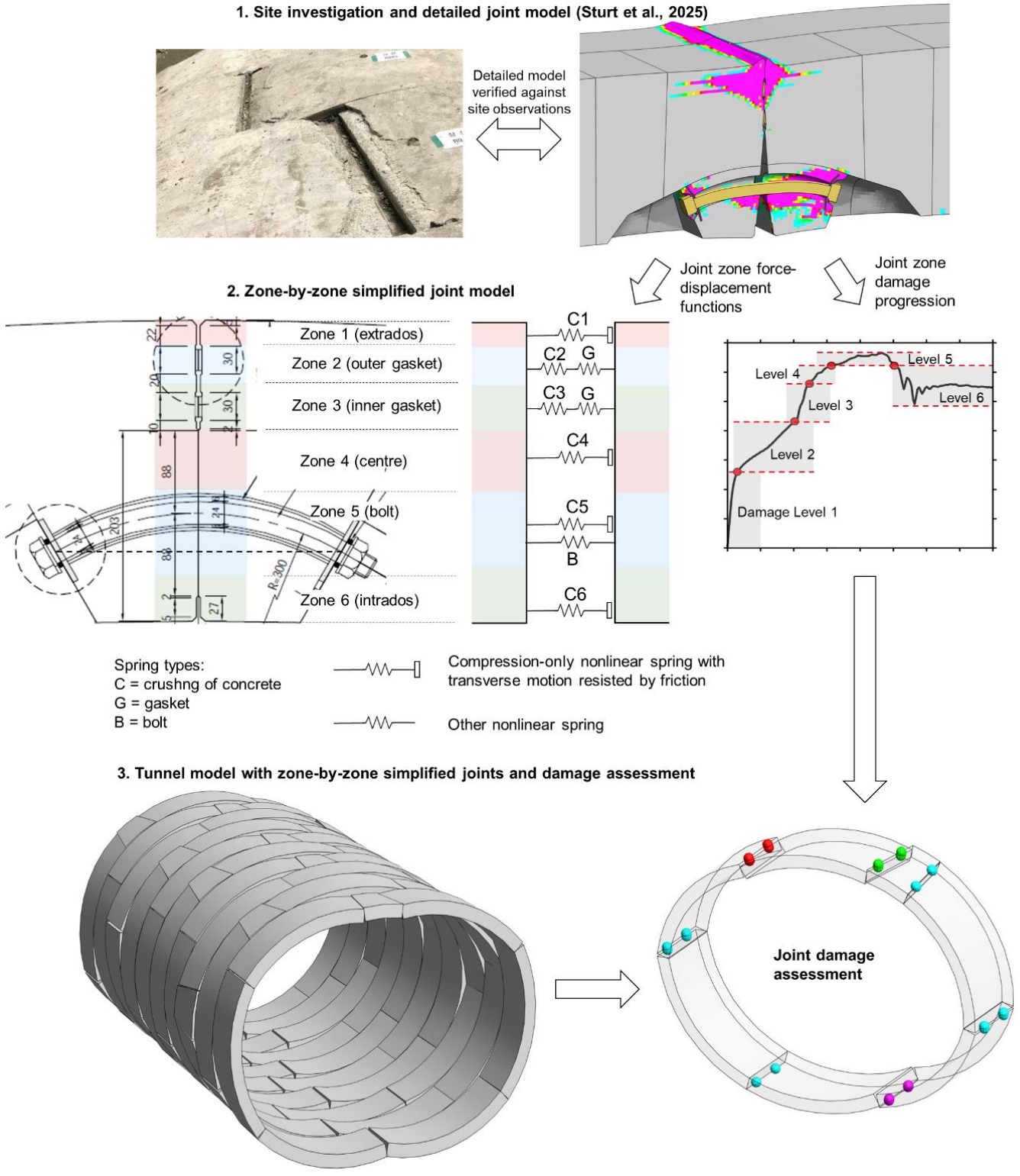

Figure 1: Logic flow for analysis of NakDong Tunnel.

2. SIMPLIFIED JOINT MODEL

2.1 JOINT MODELLING APPROACH

Previous studies have represented each joint using a single spring-like discrete element with complex force-dependent moment–rotation behaviour (Peña, 2019; Zheng, 2023). However, this approach was considered unsuitable for simulating the NakDong Tunnel, given the complex joint response revealed by the detailed finite element models. Since joint nonlinearity arises from the interaction of localised mechanisms such as concrete crushing, bolt yielding and gap closure, each mechanism is modelled separately. In this study, each joint is represented by nine nonlinear spring-like discrete elements distributed through the segment thickness, each corresponding to a specific joint face zone or component (Figure 1 centre-left diagrams). Joint face geometry is presented in Sturt et al., 2025. The detailed finite element model is "instrumented" so that forces and relative displacements can be measured separately for each joint face zone, enabling independent derivation of normal and shear force–displacement relationships for each zone. Models of both radial and circumferential joints are derived in this manner.

Joint shear resistance is provided primarily by friction at concrete contact zones, while gasket elements are assumed to provide no shear resistance, consistent with site observations. Additional post-slip resistance is provided by the bolt element, which represents shear transfer through the bolt itself and, for circumferential joints, through direct segment contact once the concrete shear key engages.

2.2 JOINT DAMAGE ASSESSMENT

Joint damage states predicted by the detailed finite element model may be mapped to the simplified model using the deformations of the joint face zones, which correspond directly to the discrete elements. In the NakDong Tunnel model, specific discrete-element deformations correspond to identifiable damage events such as seal groove closure, cracking and spalling. Progression of damage with increasing ovalisation is characterised using six generic levels (Figure 1 centre-right graph). The boundaries between damage levels are defined at points where the moment–rotation or shear force–displacement responses change gradient, typically corresponding to physically meaningful events such as contact, cracking or failure. The evolution of damage in the simplified model can be clearly visualised by plotting damage-state colours on the joint elements (Figure 1 bottom-right image).

2.3 VALIDATION OF SIMPLIFIED JOINT MODEL

The simplified joint model is validated by comparison with detailed finite element model results for identical model set-up and loading conditions; examples are shown in Figure 2. Results for rotation and shear are presented in Figure 3**,** including validation under halved joint compression force. Close matches of overall moment-rotation and force-displacement responses between detailed and simplified joint models are obtained. Furthermore, a close correspondence is obtained for the rotation angle or shear displacement at which key events are predicted to occur (such as spalling of cover concrete).

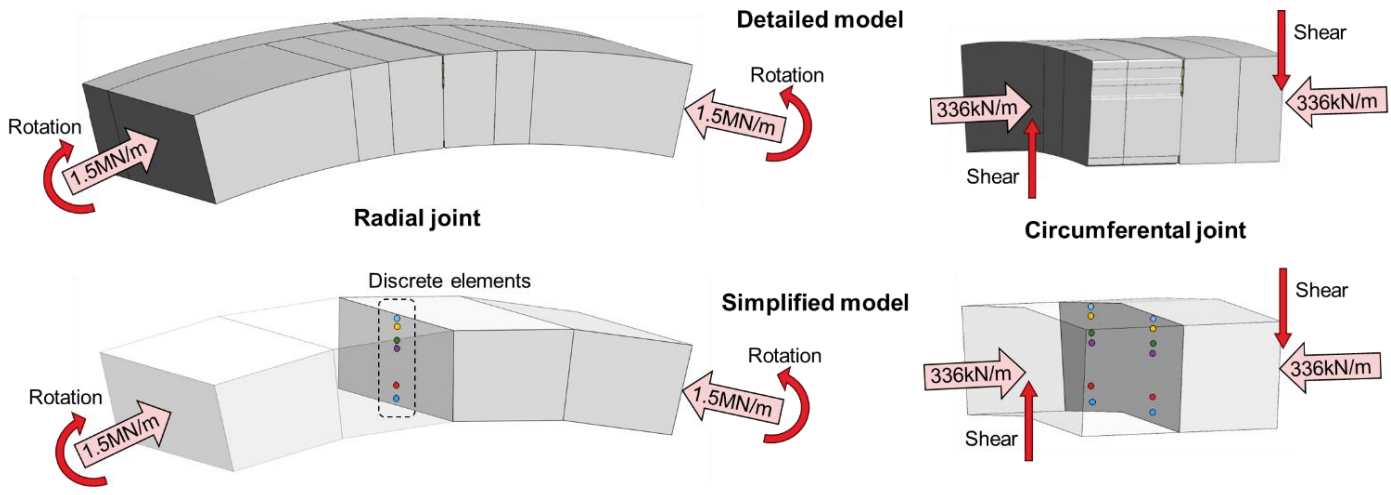

Figure 2: Set-up of simplified joint models for comparison against detailed models.

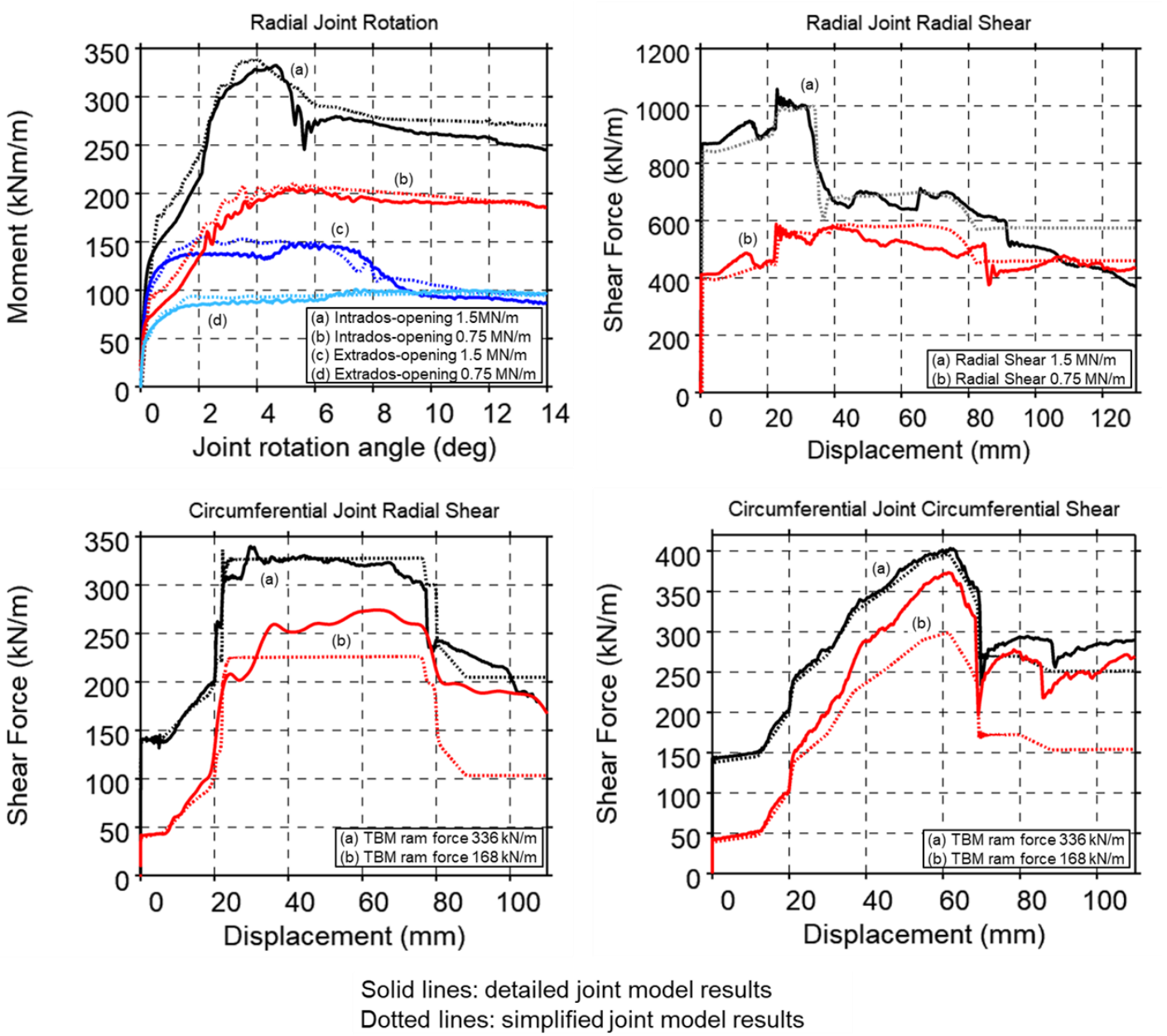

Figure 3: Simplified joint model validation results.

3. SIMPLIFIED MULTIPLE RING TUNNEL MODEL

3.1 TUNNEL LINING

The simplified joints have been included in a multiple-ring tunnel model constructed as illustrated in Figure 4. The geometry of the key segments and the staggered joint pattern are represented in the model. The segments are meshed with 0.5m x 0.8m 8-node "Thick Shell" elements in which the forces and moments are summed from stresses in a stack of six membrane-like layers subdividing the 0.32m thickness. The nonlinear constitutive model adopted, known as *MAT_CONCRETE_EC2, is specific to reinforced concrete. The input properties are 58MPa compressive strength (mean value for C50 concrete, CEN 2004) and 1.5% reinforcement ratio treated as smeared uniformly. This approach enables modelling of gross flexural failure of the segments themselves, while deformation local to the joints is modelled by the discrete elements.

For a typical staggered joint arrangement, the action of the segments under ovalising loading can be seen in the bottom-left of Figure 1.

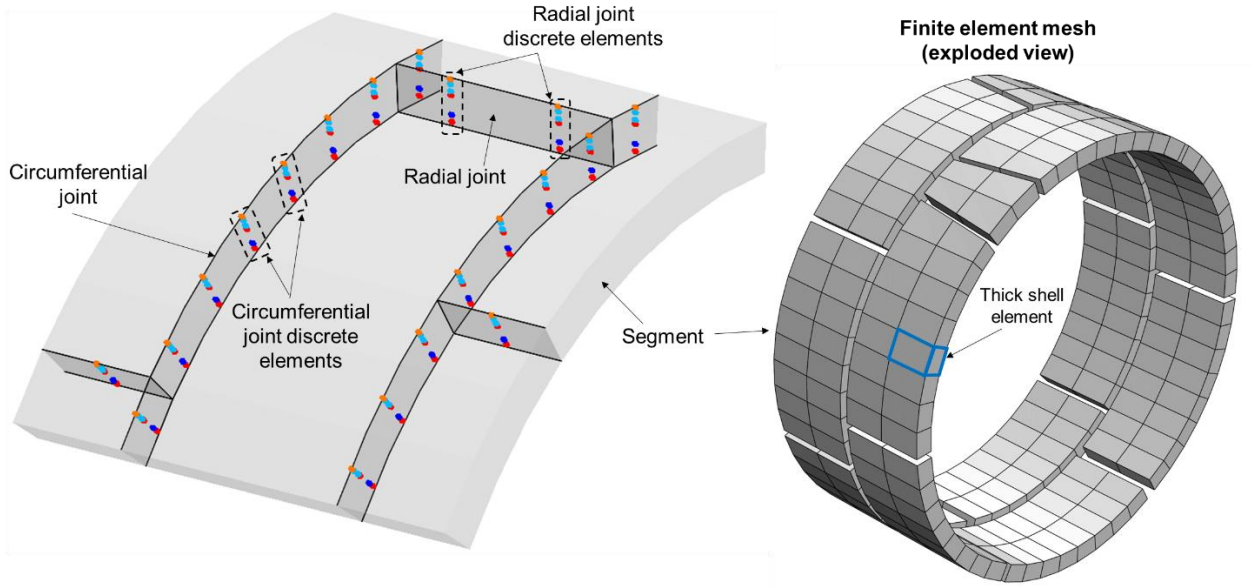

Figure 4: Simplified tunnel model construction.

3.2 SOIL MODEL AND LOADING CONDITIONS

The objective of the model is to explore the behaviour of the tunnel at large ovalising deformation, which occurs when there is a large difference between the vertical and horizontal stresses imposed on the tunnel by the surrounding soil (termed *stress difference* herein).

In the present model the surrounding soil is treated as shown in Figure 5. The soil stiffness is represented by radially oriented compression-only spring elements grouped such that different properties can be assigned to "horizontal" and "vertical" springs. Vertical and horizontal stresses (σ_V and σ_H respectively) are applied to the lining extrados surface. The upward loading on the underside of the tunnel is $\sigma_V + W$ where W balances the weight of the tunnel.

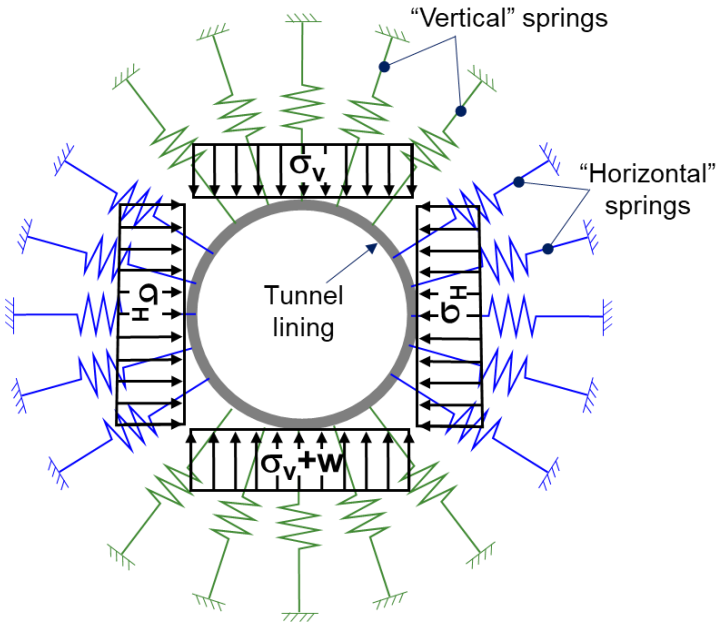

Figure 5: Soil loading model.

The spring stiffness value is derived from a calibration process between predicted and measured tunnel deformations immediately following construction; it corresponds to a soil Young's Modulus of 16.3MPa.

A gradually increasing stress difference is applied by reducing the horizontal stress σ_H while holding σ_V constant. This is intended to represent the process by which soil erosion reduced the horizontal support for the NakDong Tunnel. The rate of reduction of σ_H is displacement-controlled so as to obtain a constant

rate of shortening of the vertical diameter (which is taken as an average across the eleven rings modelled). In the example analyses presented in 3.4 below, the soil spring stiffness is held constant during each analysis for simplicity, but it is also possible to reduce the stiffness to represent the effects of erosion.

3.3 VALIDATION AGAINST SITE MEASUREMENTS

The absence of quantitative information on in-situ soil stress conditions prevents validation of the model's primary output, namely ovalising deformation as a function of nett stress difference. However, secondary measurements, including cross-section shape and joint deformation at given levels of ovalisation, were compared with site measurements from intact but deformed sections of the tunnel.

Following removal of most soil debris from the Upline tunnel, Rings 1077 to 1223 were selected for study due to their relatively large deformation (150–200 mm squatting). A LiDAR survey was carried out to generate a 3D interior surface model (Figure 6). Cross-sections were extracted from both the survey data and the numerical model at rings with matching key segment positions (Figure 7), with model results taken at snapshots corresponding to the same squatting deformation as measured on site.

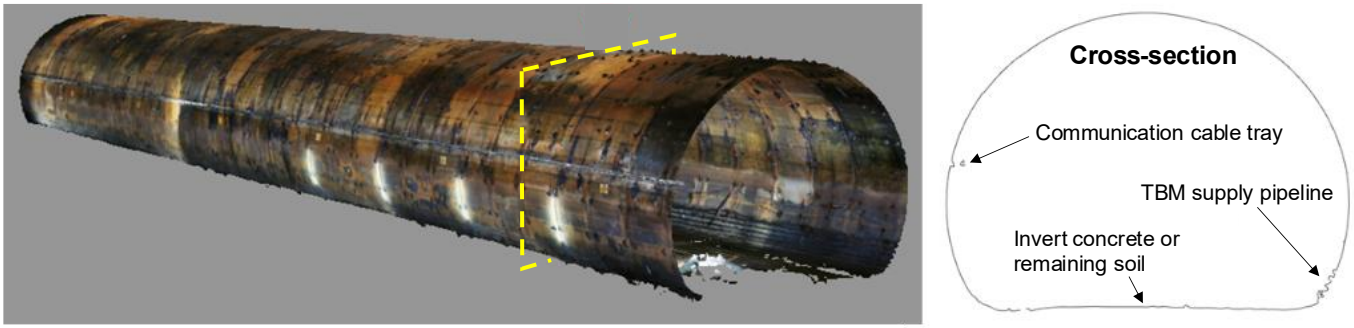

Figure 6: 3D interior surface model from LiDAR survey with typical cross-section.

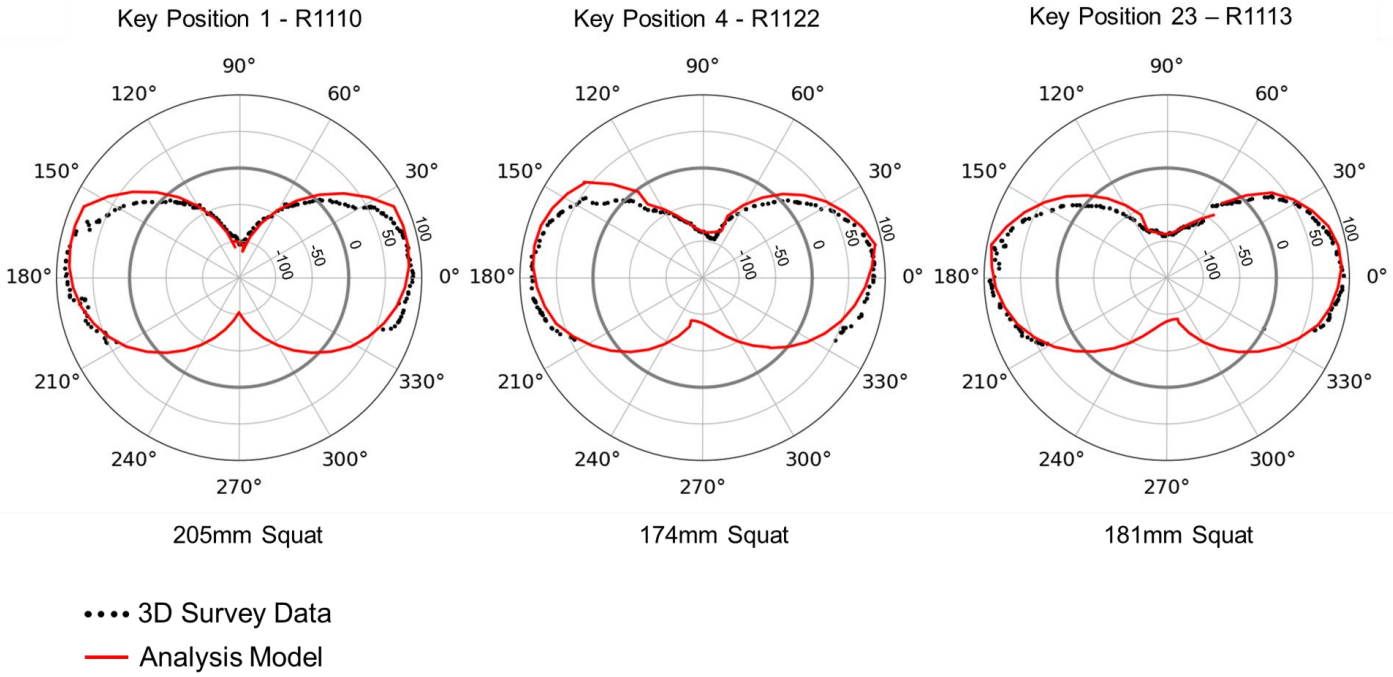

Figure 7: Radial deformation (mm) of Rings 1110, 1122 and 1113.

Joint slip (step-like displacement across a joint) was measured at seven rings between R1042 and R1050 and compared with numerical results obtained at the same level of overall tunnel deformation (Figure 8, Table 1). The numerical results shown were obtained with the longitudinal force in the tunnel, which influences slip of circumferential joints but has an unknown real-life value, set to 224 kN/m (40% of TBM ram force).

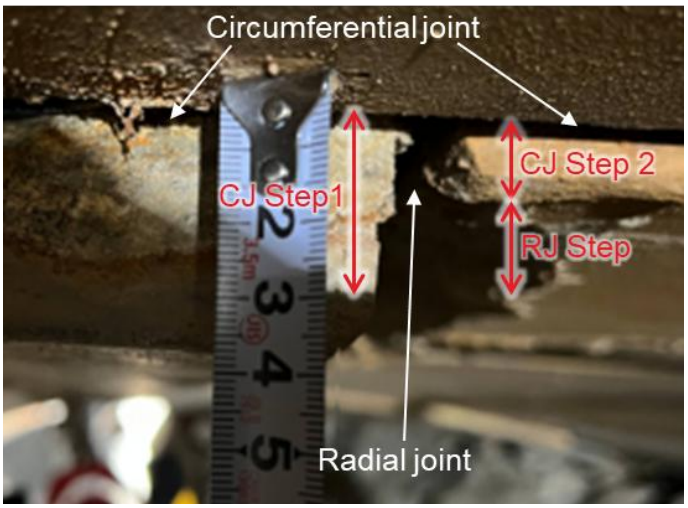

Figure 8: Step measurements at tunnel crown.

Table 1: Joint step sizes

Joint step	Site measurement (mm)	Analysis (mm)
Circumferential Joint (average of 14 measurements)	25	23
Radial Joint (average of 7 measurements)	18	10

3.4 INFLUENCE OF CIRCUMFERENTIAL JOINT DESIGN ON OVALISATION RESPONSE

As an example of how the proposed joint modelling methodology can be used in design studies, it has been applied to investigate the sensitivity of tunnel ovalisation resistance to the details of the circumferential joints. These joints stiffen the ovalisation response by forcing neighbouring rings to adopt similar deformation shapes despite differing radial joint positions, with the magnitude of this effect depending on circumferential joint stiffness (Figure 9). At low levels of ovalisation, shear transfer between rings occurs primarily through friction, with little slip irrespective of joint details. Once friction capacity is exceeded, the response depends on joint design. The circumferential joints of the NakDong Tunnel are relatively flexible in this regime due to curved bolts and clearance gaps. By contrast, segmental tunnels that are designed with dowelled circumferential joints and minimal clearance gaps exhibit a stiffer joint response but greater forces on the connectors.

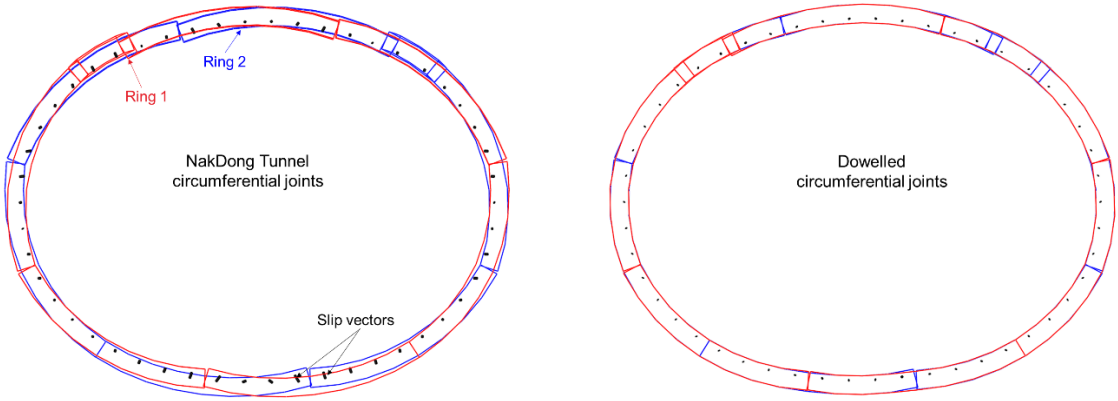

Figure 9: Circumferential joint slip vectors at 150mm ovalisation, deformation shown magnified.

The influence of circumferential joint design on ovalisation response is shown in Figure 10. Idealised infinitely strong dowels cause all rings to deform almost identically and increase stiffness at intermediate deformation levels by up to 13% but have little effect on ultimate nett stress difference or deformation capacity compared to the actual bolted joint detail. Removing all circumferential joint shear resistance

enables each ring to ovalise independently, reducing ultimate nett stress difference capacity by 44% and deformation capacity by 42%.

Comparison of the response curves in Figure 10 shows that, within the normal design deformation range (up to about 100 mm ovalisation), friction has a greater influence than bolts or shear keys, increasing both the initial ovalising stiffness and the yield deformation by approximately 20%. Reduced joint friction, for example due to the use of bituminous or plywood pads, would result in behaviour between the baseline and frictionless cases.

For the idealised infinitely strong dowels, shear forces in the dowels up to 574kN are predicted prior to reaching the maximum ovalisation deformation ($\Delta D = 364mm$). However, such large forces exceed the capacity of dowels commonly available on the market, which is typically of the order of 400kN.

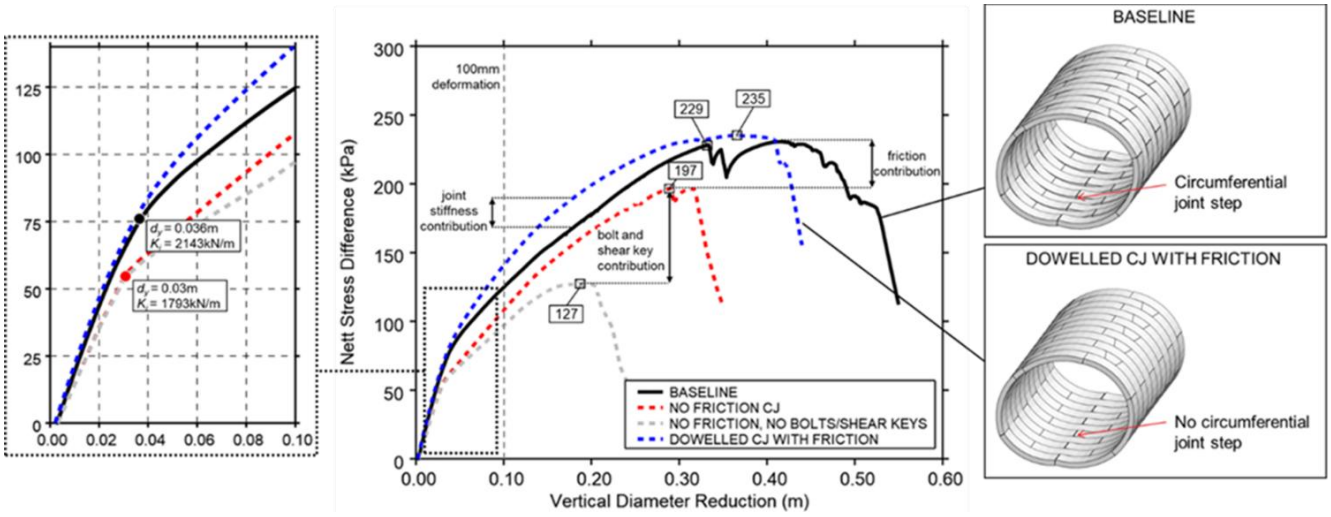

Figure 10: Sensitivity of stress difference response to circumferential joint stiffness and friction properties.

4. CONCLUSIONS

A numerical modelling method is proposed in which the joints of segmental tunnel linings are represented by a series of spring-like discrete elements distributed through the segment thickness, each representing a particular zone of the joint face or a component such as a bolt or gasket. The nonlinear force–displacement properties of the discrete elements are informed by detailed finite element models of the radial and circumferential joints. Joint damage progression can be interpreted directly from discrete-element deformations.

The proposed joint modelling methodology was applied in a multi-ring model of the NakDong Tunnel with staggered joint pattern. Cross-section deformed shapes and joint step displacements predicted by the models were compared against measurements at the collapse site, showing good agreement of results. Example analyses are presented that explore the influence of circumferential joint design on tunnel ovalisation response. At low deformation levels, shear transfer is governed mainly by friction, with little relative slip regardless of joint detailing. Once friction is exceeded, the connectors play an important role in increasing the tunnel's deformation capacity prior to collapse, and this remains true irrespective of whether bolts or dowels are used.

5. ACKNOWLEDGEMENTS

The authors gratefully acknowledge the permission granted by SK ecoplant Co., Ltd. to publish project data and photos.

LITERATURE

Ansys, 2024. LS-DYNA Keyword User's Manual, LS-DYNA R15. *Ansys inc,* 2024

CEN 2004. Eurocode 2: Design of concrete structures, EN 1992-1-1:2004+A1:2014. Ed: CEN/TC 250.

Moreno-Martinez, J., Galván, A., Peña, F., and Carpio, F., 2020. Practical Model Proposed for the Structural Analysis of Segmental Tunnels. *Applied Sciences. 10(23),* p.8514.

Peña, F., Galván, A., Moreno-Martínez, J.Y. and Herrera-Díaz, I.E., 2019. Moment–rotation behaviour of non-bolted planar joints for segmental tunnels. *Proceedings of the Institution of Civil Engineers-Structures and Buildings, 172(10)*, pp.749-767.

Seol, H., Won, D., Jang, J., Kim, K.Y. and Yun, T.S., 2022. Ground Collapse in EPB shield TBM site: A case study of railway tunnels in the deltaic region near Nak-Dong River in Korea. *Tunnelling and Underground Space Technology, 120,* p.104274.

Sturt, R., Montalbini, G., and Jung, H-I., 2025. The behaviour of segmental tunnel linings beyond their typical design limit of ovalisation: site investigation of a collapsed tunnel and detailed joint modelling. *Tunnelling and Underground Space Technology, 162, p.106676.*

Wood, A.M., 1975. The circular tunnel in elastic ground. *Géotechnique, 25(1)*, pp.115-127.

Richard Sturt
Arup, UK
Richard.Sturt@arup.com

Gianmarco Montalbini
Arup, UK
Gianmarco.Montalbini@arup.com

Hyuk-Il Jung
Arup, UK
Hyuk-Il.Jung@arup.com